Electronic Supplementary Material (ESI) for Journal of Materials Chemistry C.

Highly efficient blue electroluminescence based on TADF emitter with spiro acridine donor: methyl group effect on photophysical properties

Han Xia,[a‡], Yukun Tang[b‡] Youming Zhang,[a‡] Fan Ni,*[c] Yuntao Qiu,[a] Chih-Wei Huang,[b] Chung-Chih Wu,*[b] Chuluo Yang*[a]

[a] Guangdong Research Center for Interfacial Engineering of Functional Materials, College of Materials Science and Engineering, Shenzhen University, Shenzhen 518060, P. R. China.
[b] Department of Electrical Engineering, Graduate Institute of Electronics Engineering and Graduate Institute of Photonics and Optoelectronics, National Taiwan University, Taipei, 10617, Taiwan.
[c] School of Instrument Science and Optoelectronics Engineering, Department of Biomedical Engineering, Hefei University of Technology, Hefei 230009, P. R. China.
[‡] H. Xia, C-W Huang and Y. Zhang contributed equally to this work.

Corresponding author: Dr. Fan Ni; Prof. Chuluo Yang; Prof. Chung-Chih Wu.

Email address: nfope@hfut.edu.cn; clyang@szu.edu.cn; f05941059@ntu.edu.tw.

General information

4,4'-sulfonylbis(chlorobenzene) and 4,4'-sulfonylbis(1-bromo-2-methylbenzene) were purchased and were directly used without further purification.

The ^{1}H nuclear magnetic resonance (NMR) spectra were recorded in chloroform ($CDCl_3$) or dimethylsulphoxide (DMSO) solution on a 500 MHz Bruker NMR spectrometer with tetramethylsilane (TMS) as the internal standard. High-resolution mass spectra (HR-MS) were conducted on Thermo Scientific LTQ Orbitrap XL.

Thermogravimetric analysis (TGA) was performed on a TGA-Q50 Instrument (TA Instruments, America) with a heating rate of 20 ^{o}C/min from 50 to 750 ^{o}C under a nitrogen atmosphere.

UV-vis absorption spectra were obtained on a Shimadzu UV-2600 spectrophotometer (Shimadzu, Japan) at room temperature. Photoluminescence (PL) spectra were measured on a Hitachi F-7100 fluorescence spectrophotometer (Hitachi, Japan). The transient PL decays were measured by a single photon counting spectrometer (Picoquant, FluoTime 300, Germany). The solid state absolute photoluminescence quantum yields (PLQYs) were measured on a Hamamatsu UV-NIR absolute PL quantum yield spectrometer (C13534, Hamamatsu Photonics) equipped with a calibrated integrating sphere under argon atmosphere. Cyclic voltammetry (CV) measurements were carried out on a CHI600 electrochemical analyzer (Chenhua, China) at room temperature, with a conventional three-electrode system consisting of a glassy carbon working electrode, a platinum wire auxiliary electrode, and an Ag/AgCl reference electrode. Dichloromethane and tetrabutylammonium hexafluorophosphate ($TBAPF_6$) (0.1 M) were used as the solvent and supporting electrolyte, respectively. The sweep speed was set as 100 mV s^{-1}.

The geometrical and electronic properties of the ground state molecules were performed using B3LYP/6-31G(d,p) level of theory. PBE0/def2-SVP theory was used for the calculation of energy gap between the S_1 and T_1 states. The B3LYP/def2-SVP level was used in the configuration calculation of S_1 state.

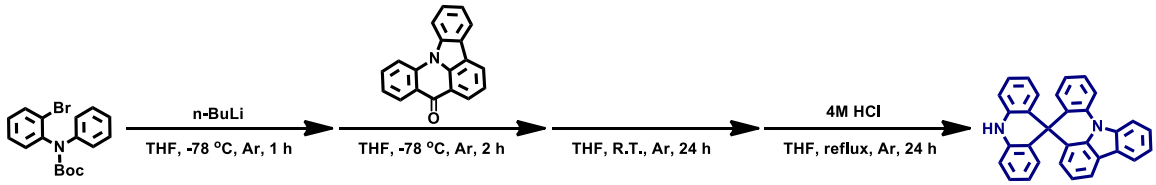

Scheme S1. The synthetic route for SAIA

The synthesis of 10*H*-spiro[acridine-9,8'-indolo[3,2,1-de]acridine] (SAIA)

In a dry three-neck flask, 1.6 M n-BuLi in hexane (4 mL, 6.4 mmol) was added dropwise to a solution of *tert*-butyl (2-bromophenyl)(phenyl)carbamate (2.16 g, 6.2 mmol) in 30 mL dry THF at −78 °C under argon. After stirring the mixture for 1 h at this temperature, 8*H*-indolo[3,2,1-de]acridin-8-one (1.67 g, 6.2 mmol) in 80 mL dry THF was added dropwise into the mixture with stirring for 2 h and then stirred the mixture for 24 h at the room temperature. The jet-black mixture was added 10 mL 4M HCl at once and then warmed to reflux. After 24 h, the red mixture was concentrated by using a rotary evaporator. Then the concentrated mixture was poured into water (100 mL) and further extracted with CH_2Cl_2 (100 mL × 3). The collected CH_2Cl_2 solution was died with anhydrous Na_2SO_4 and concentrated under vacuum. The crude compound were purified by silica gel column chromatography to obtain a white solid (965 mg, 2.29 mmol) with a yield of 37%.

^{1}H NMR (500 MHz, DMSO-d_6, δ): 9.26 (s, 1H), 8.44 (d, J = 8.5 Hz, 1H), 8.30 (t, J = 8.0 Hz, 2H), 7.97 (d, J = 7.5 Hz, 1H), 7.64 (t, J = 7.5 Hz, 1H), 7.41 (t, J = 7.5 Hz, 1H), 7.35 (t, J = 8.5 Hz, 1H), 7.21 (t, J = 7.5 Hz, 1H), 7.13 (d, J = 8.0 Hz, 1H), 7.05-6.99 (m, 3H), 6.95-6.91 (m, 3H), 6.53-6.50 (m, 4H). ^{13}C NMR (125 MHz, DMSO-d_6, δ): 138.1, 137.0, 136.6, 134.3, 134.0, 133.3, 131.64, 131.60, 129.2, 128.1, 127.7, 127.6, 127.0, 125.8, 124.1, 123.4, 121.8, 121.6, 121.5, 120.3, 118.1, 114.3, 114.2, 114.1, 47.3, 40.6, 40.5, 40.4, 40.3, 40.24, 40.15, 39.98, 39.81, 39.7, 39.5. HRMS (ESI, m/z): $[M+H]^+$calcd for $C_{31}H_{21}N_2^+$: 421.1700; found: 421.1694.

The synthesis of 10,10''-(sulfonylbis(4,1-phenylene))bis(10*H*-spiro[acridine-9,8'-indolo[3,2,1-de]acridine]) (DPS-SAIA)

To a 100 mL flask was added $Pd(OAc)_2$ (0.015 g, 0.064 mmol), *t*-BuONa (0.37 g, 3.84 mmol), $(t\text{-}Bu)_3PHBF_4$ (0.056 g, 0.192 mmol), 10*H*-spiro[acridine-9,8'-indolo[3,2,1-de]acridine] (1.48 g, 3.52 mmol) and 4,4'-sulfonylbis(chlorobenzene) (0.459 g, 1.6 mmol). The mixture was refluxed in 30 mL of freshly distilled toluene under an argon atmosphere for 24 h. The reaction mixture was cooled to room temperature, and the solvent was evaporated under vacuum. The target compound was obtained as a white solid (1.22 g, 1.152 mmol) after passing through the column of neutral alumina with a yield of 72%.

^{1}H NMR δ_H (500 MHz, $CDCl_3$): δ_H (500 MHz, $CDCl_3$) : 8.45 (d, *J* = 8.5 Hz, 4H), 8.29 (d, *J* = 8.5 Hz, 2H), 8.21 (t, *J* = 8.5 Hz, 4H), 7.88 (d, *J* = 7.5 Hz, 2H), 7.79 (d, *J* = 8.5 Hz, 4H), 7.63 (t, *J* = 8.5 Hz, 2H), 7.41 (t, *J* = 7.5 Hz, 2H), 7.38-7.33 (m, 4H), 7.24 (d, *J* = 7.5 Hz, 2H), 7.17 (d, *J* = 7.5 Hz, 2H), 7.04 (t, *J* = 8.0 Hz, 2H), 6.91 (t, *J* = 8.5 Hz, 4H), 6.87 (d, *J* = 7.5 Hz, 4H), 6.66 (t, *J* = 8.0 Hz, 4H), 6.26 (d, *J* = 8.0 Hz, 4H). HRMS (ESI, m/z): $[M+Na]^+$ calcd for $C_{74}H_{46}N_4O_2SNa^+$: 1077.3234; found: 1077.3230.

The synthesis of 10,10''-(sulfonylbis(2-methyl-4,1-phenylene))bis(10*H*-spiro[acridine-9,8'-indolo[3,2,1-de]acridine]) (Me-DPS-SAIA)

To a 100 mL flask was added $Pd_2(dba)_3$ (0.074 g, 0.08 mmol), *t*-BuONa (0.338 g, 3.52 mmol), (*t*-Bu)$_3$PHBF$_4$ (0.023 g, 0.08 mmol), 10*H*-spiro[acridine-9,8'-indolo[3,2,1-de]acridine] (1.48 g, 3.52 mmol) and 4,4'-sulfonylbis(1-bromo-2-methylbenzene) (0.646 g, 1.6 mmol). The mixture was refluxed in 30 mL of freshly distilled toluene under an argon atmosphere for 24 h. The reaction mixture was cooled to room temperature, and the solvent was evaporated under vacuum. The target compound was obtained as a white solid (1.09 g, 1.01 mmol) after passing through the column of neutral alumina with a yield of 63%.

^{1}H NMR δ_H (500 MHz, $CDCl_3$): δ_H (500 MHz, $CDCl_3$) : 8.31-8.28 (m, 4H), 8.24-8.19 (m, 6H), 7.88 (t, *J* = 7.5 Hz, 2H), 7.68 (d, *J* = 8.0 Hz, 2H), 7.63 (t, *J* = 8.0 Hz, 2H), 7.41 (t, *J* = 7.5 Hz, 2H), 7.37-7.30 (m, 4H), 7.24 (d, *J* = 7.5 Hz, 2H), 7.17 (d, *J* = 7.5 Hz, 1H), 7.09 (d, *J* = 7.5 Hz, 1H), 7.06-7.02 (m, 2H), 6.93-6.88 (m, 8H), 6.65 (t, *J* = 7.5 Hz, 4H), 6.12 (d, *J* = 8.5 Hz, 4H), 2.434 (s, 3H), 2.427 (s, 3H). HRMS (ESI, m/z): $[M+Na]^+$ calcd for $C_{76}H_{50}N_4O_2SNa^+$: 1105.3547; found: 1105.3557.

Device fabrication and measurements

All organic materials used in experiments (except for the TADF emitters) were purchased from Lumtec, Inc. All compounds were subjected to temperature-gradient sublimation under a high vacuum before use. OLEDs were fabricated on the ITO-coated glass substrates with multiple organic layers sandwiched between the transparent bottom indium-tin-oxide (ITO) anode and the top metal cathode. All material layers were deposited by vacuum evaporation in a vacuum chamber with a base pressure of 10^{-6} torr. The deposition system permits the fabrication of the complete device structure in a single vacuum pump-down without breaking vacuum. The deposition rate of organic layers was kept at 0.1 - 0.2 nm/s. The doping was conducted by co-evaporation from separate evaporation sources with different evaporation rates. The active area of the device is 1 ×1 mm^2, as defined by the 10 shadow mask for cathode deposition. The current-voltage-brightness (J-V-L) characterization of the light-emitting devices was performed with a source-measurement unit (SMU) and a spectroradiometer (DMS 201, AUTRONIC-MELCHERS GmbH). EL spectra of devices were collected by a calibrated CCD spectrograph. The angular dependence of EL intensities (and spectra) was measured by a calibrated goniometric spectroradiometer (DMS 201, AUTRONIC-MELCHERS GmbH). The external quantum efficiencies of devices were determined by collecting the total emission fluxes with a calibrated integrating-sphere measurement system and by measuring the angular distribution of the emission spectra and intensities.

Exciton Dynamic Rate Constant Calculation [1]

The emission quantum yields Φ_p and Φ_d for the prompt and delayed fluorescence components were determined by the following relationship:

$$\Phi_d = \frac{k_{r,S}}{k_d}\frac{k_p - k_{r,S} - k_{nr,S} - k_{ISC}}{k_p - k_d} \quad \text{.....Eq.(1)}$$

$$\Phi_p = \frac{k_{r,S}}{k_p}\frac{k_{r,S} + k_{nr,S} + k_{ISC} - k_d}{k_p - k_d} \quad \text{.....Eq.(2)}$$

Where the k_d and k_p were determined by the lifetimes of the prompt (τ_p) and delayed (τ_d) fluorescence as follows:

$$k_p = \frac{1}{\tau_p} \quad \text{.....Eq.(3)}$$

$$k_d = \frac{1}{\tau_d} \quad \text{.....Eq.(4)}$$

while $k_{r,S}$, k_{RISC}, k_{ISC} and $k_{nr,S}$ can be estimated using the following equations (Φ_{PL} indicates the total PLQY):

$$k_{r,S} = \Phi_p k_p + \Phi_d k_d \approx \Phi_p k_p \quad \text{.....Eq.(5)}$$

$$k_{nr,S} = \frac{1-\Phi_{PL}}{\Phi_{PL}} k_{r,S} = \frac{1-\Phi_{PL}}{\Phi_{PL}\tau_p}\Phi_p \quad \text{.....Eq.(6)}$$

$$k_{RISC} = \frac{k_p k_d \Phi_{PL}}{k_{r,S}} = \frac{\Phi_{PL}}{\tau_d \Phi_p} \quad \text{.....Eq.(7)}$$

$$k_{ISC} \approx \frac{k_p k_d \Phi_d}{k_{RISC}\Phi_{PL}} = \frac{\Phi_d}{\tau_p \Phi_{PL}} \quad \text{.....Eq.(8)}$$

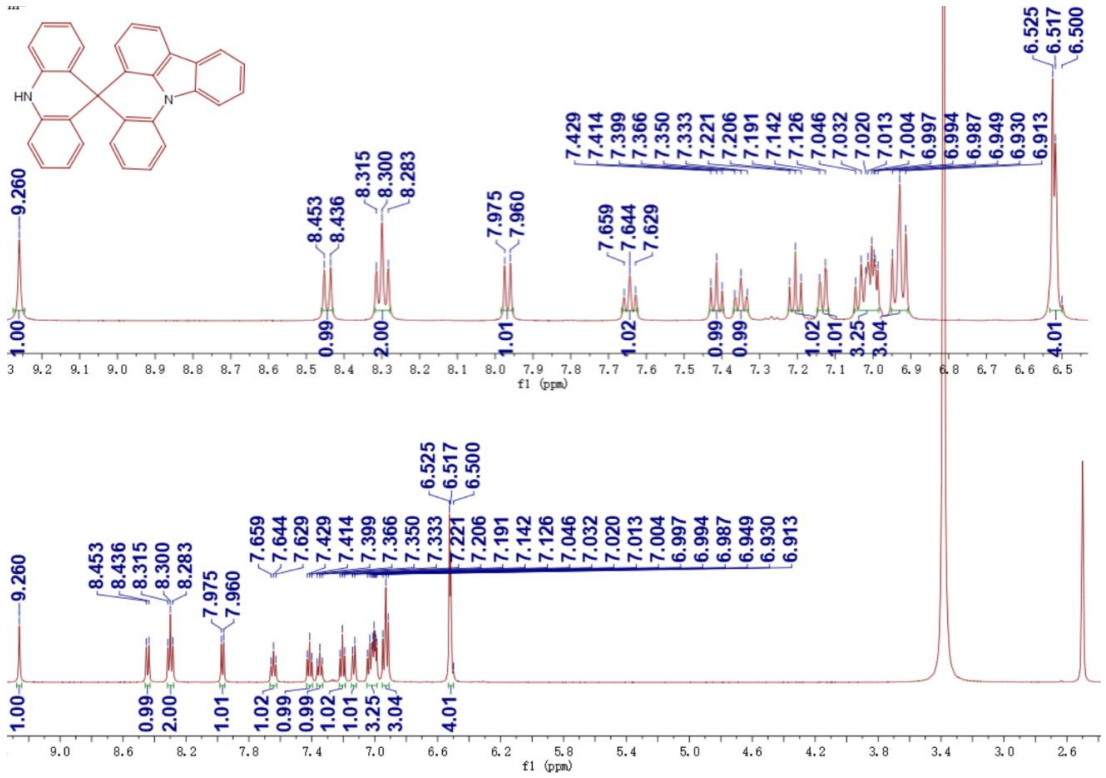

Fig. S1 ^{1}H NMR spectrum of SAIA (500 MHz, DMSO-d_6, 25 ^{o}C).

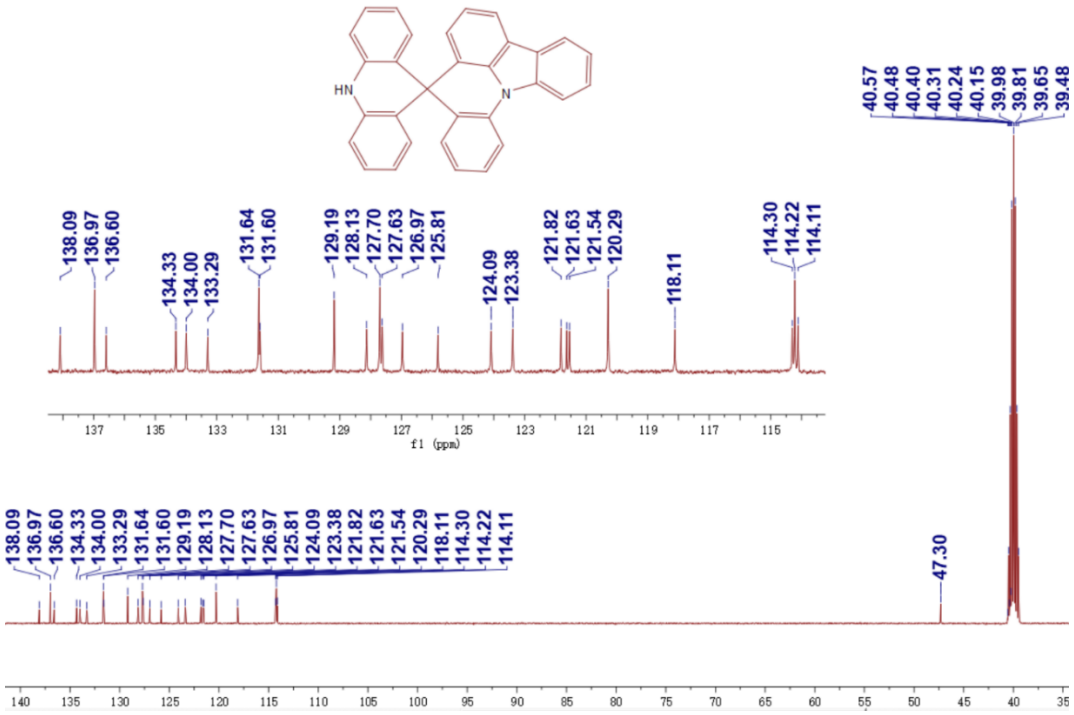

Fig. S2 ^{13}C NMR spectrum of SAIA (125 MHz, DMSO-d_6, 25 ^{o}C).

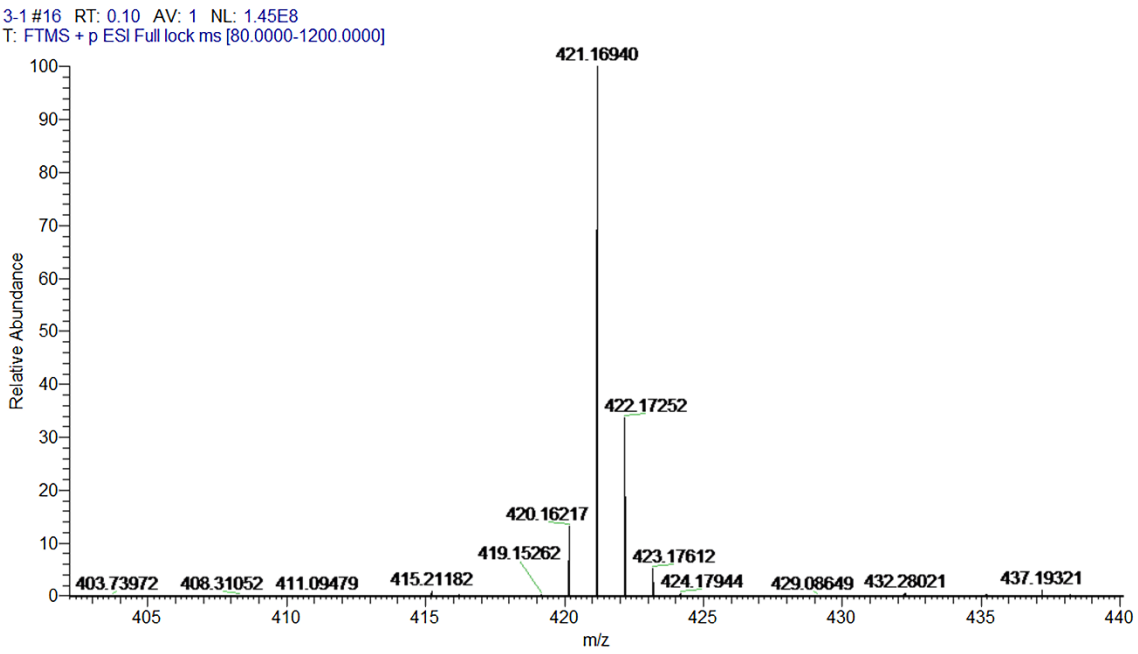

Fig. S3 High-resolution mass spectra of SAIA.

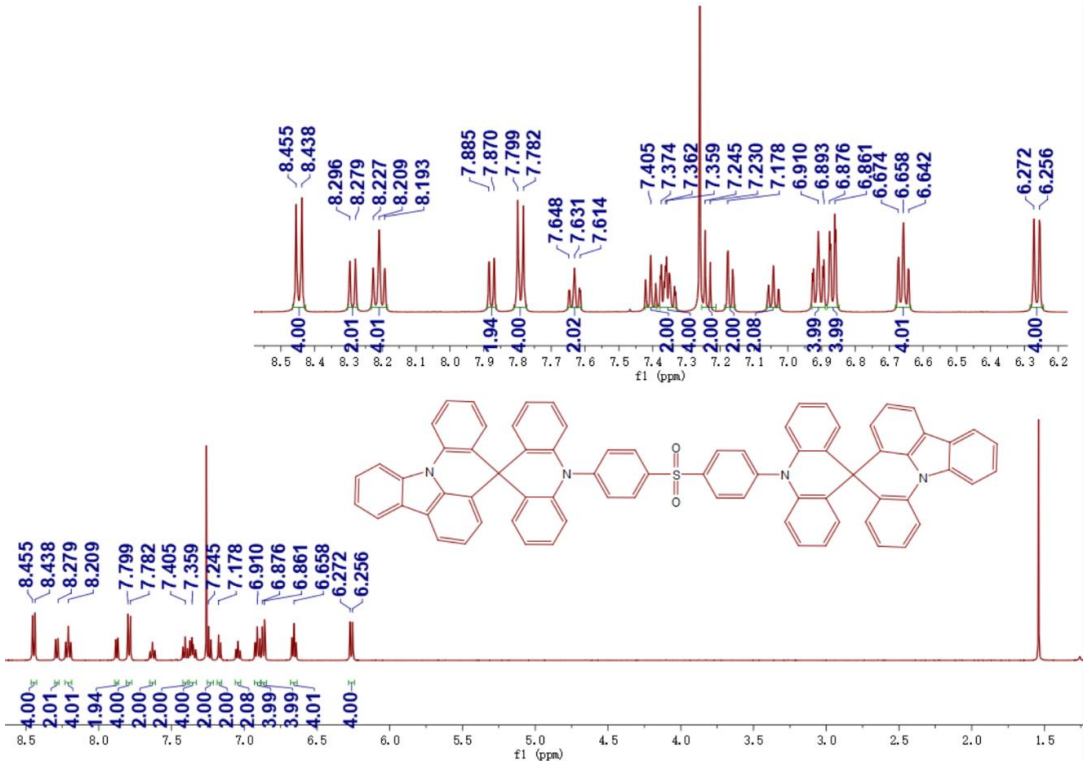

Fig. S4 ^{1}H NMR spectrum of DPS-SAIA (500 MHz, $CDCl_3$, 25 °C).

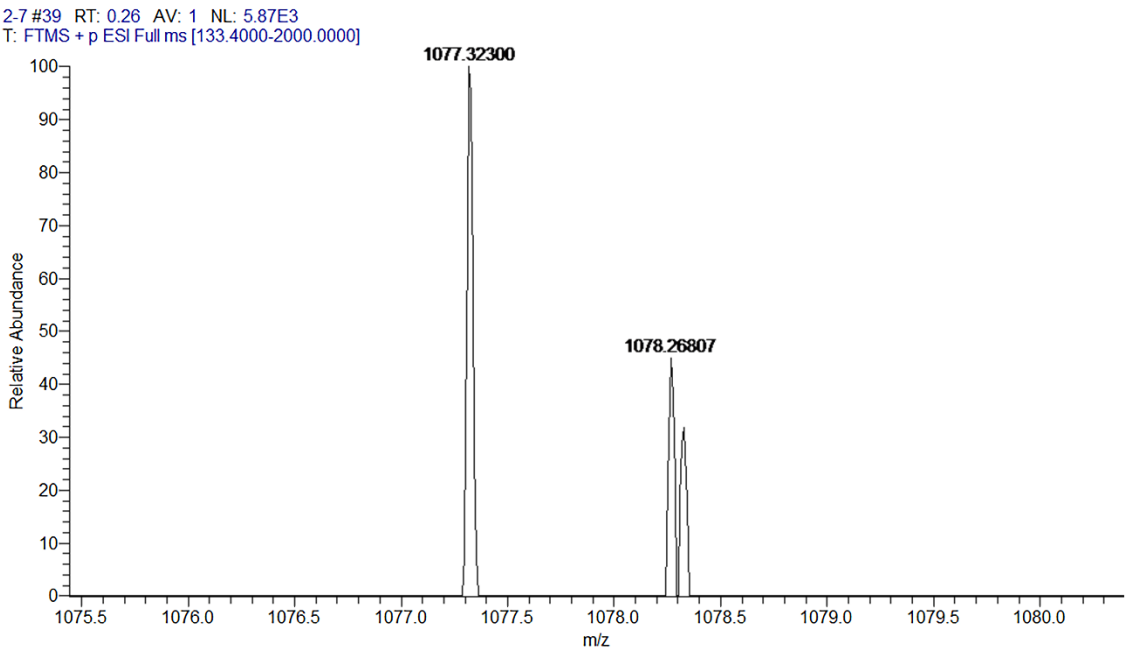

Fig. S5 High-resolution mass spectra of DPS-SAIA.

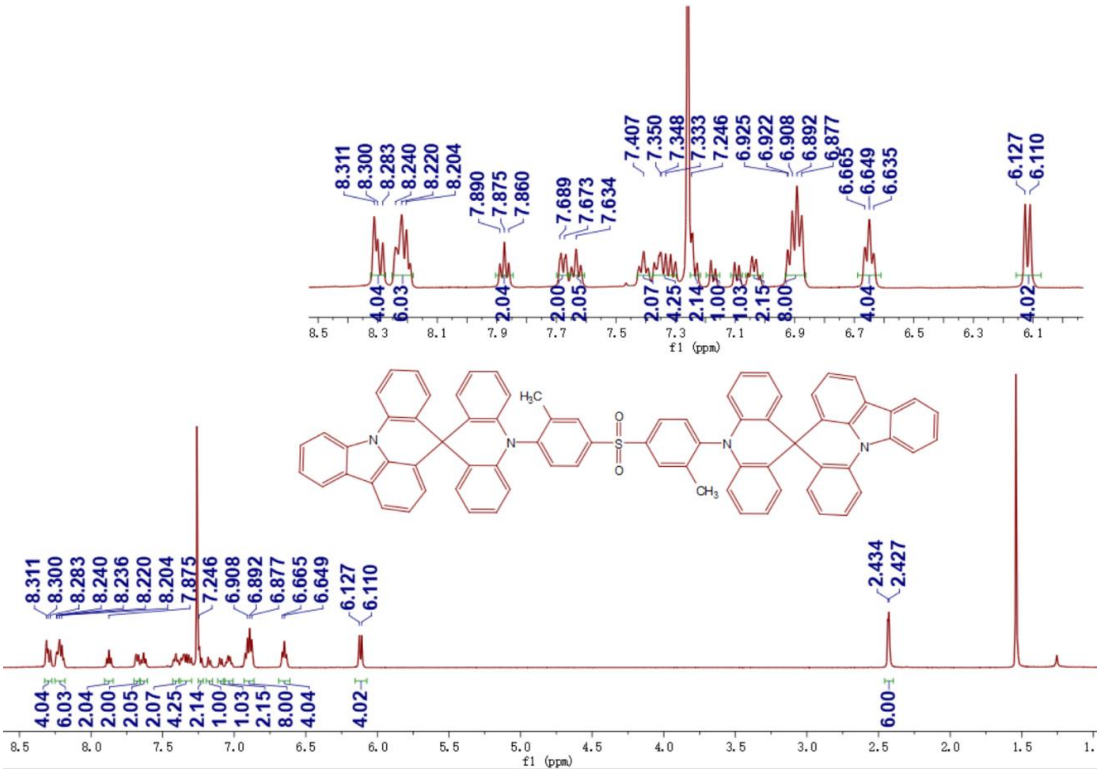

Fig. S6 ^{1}H NMR spectrum of Me-DPS-SAIA (500 MHz, $CDCl_3$, 25 ^{o}C).

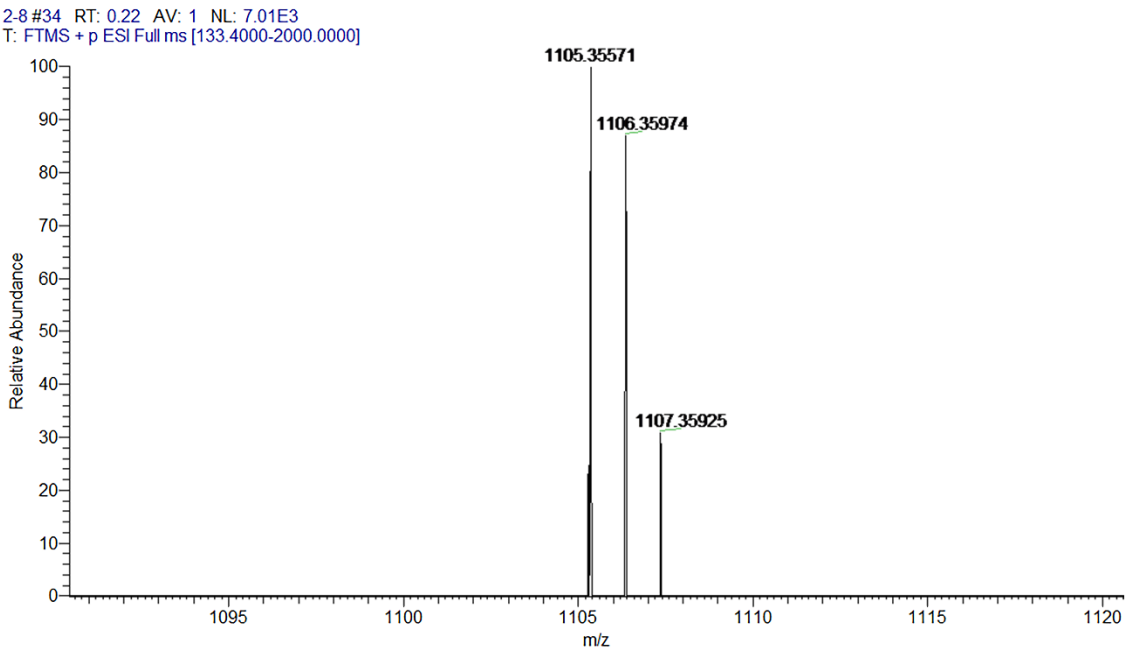

Fig. S7 High-resolution mass spectra of Me-DPS-SAIA.

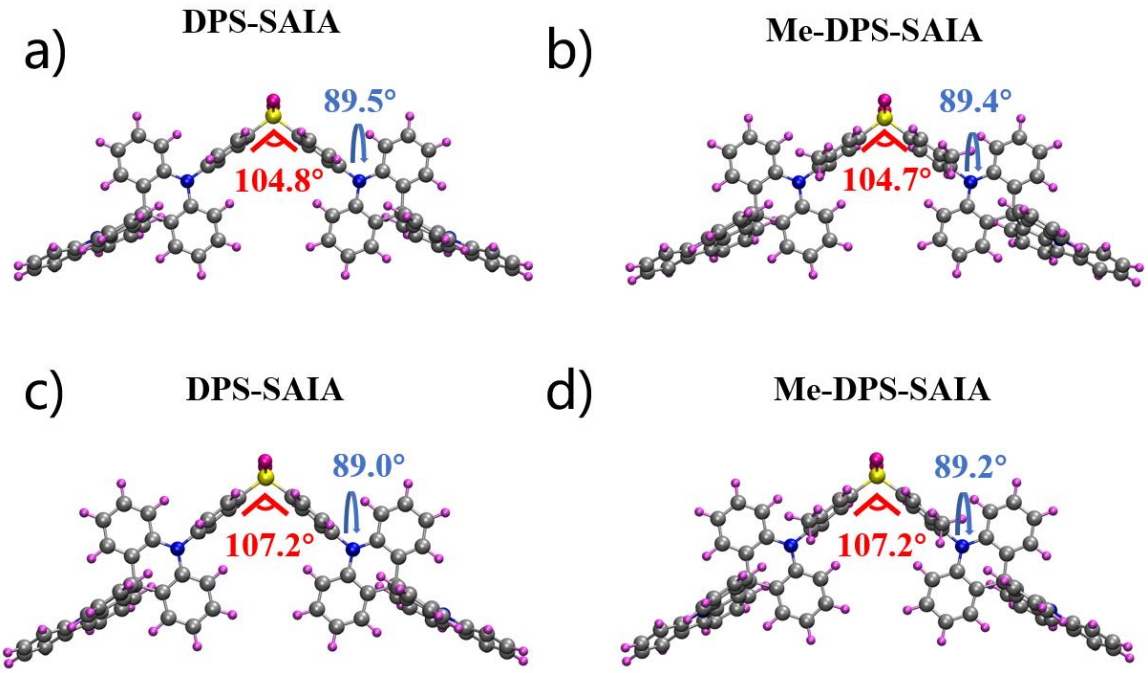

Fig. S8 The optimized ground state (a and b) and excited state (c and d) configurations of DPS-SAIA (a and c) and Me-DPS-SAIA (b and d).

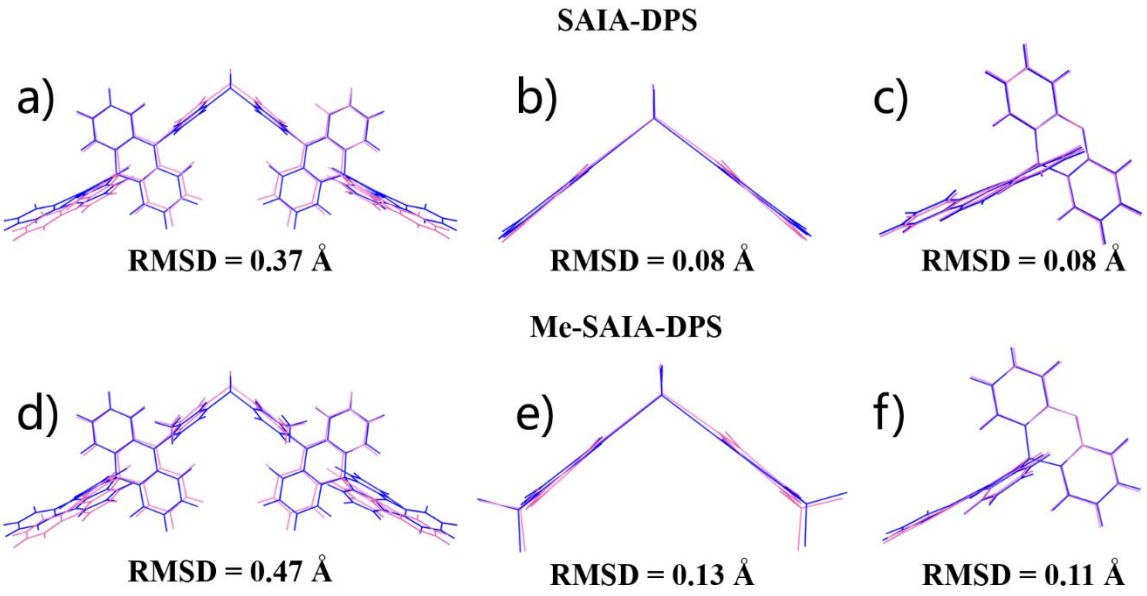

Fig. S9 Comparison of the optimized structures of SAIA-DPS(a), Me-SAIA-DPS(d), or their acceptor(b and e) and donor(c and f)in the S_0 (blue), and S_1 (pink) states.

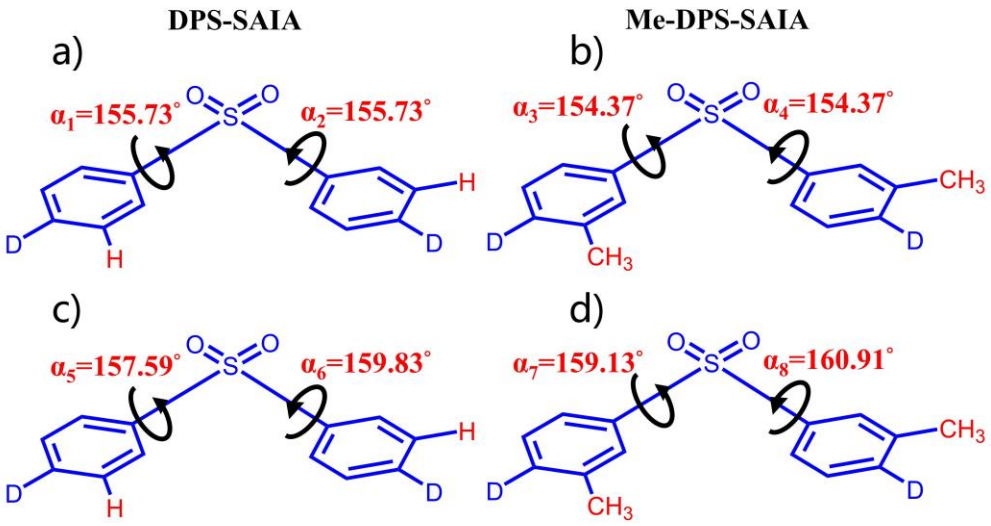

Figure S10. Two models for optimized ground state (a and b) and excited state (c and d) configurations of DPS-SAIA (a and c) and Me-DPS-SAIA (b and d). α denotes dihedral angles.

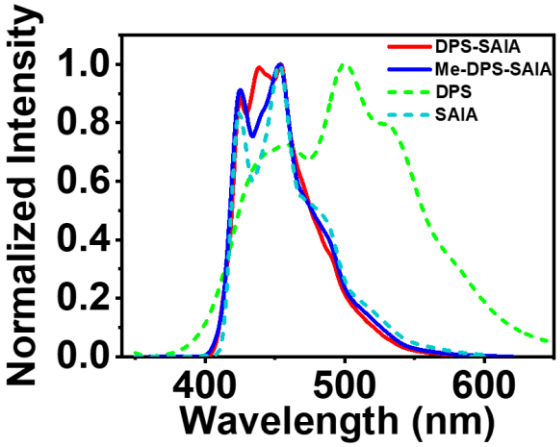

Fig. S11 The phosphorescence spectra of 10^{-5}M DPS-SAIA, Me-DPS-SAIA, DPS, and SAIA in toluene solutions at 77 K.

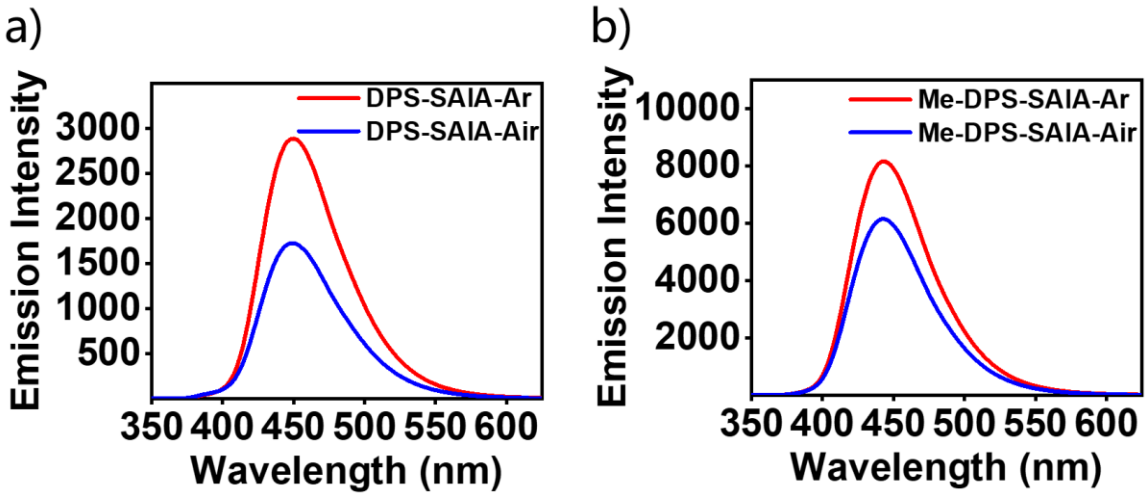

Fig. S12 The fluorescence spectra of 10^{-5} M DPS-SAIA (a) and Me-DPS-SAIA (b) in aerated and degassed toluene solutions.

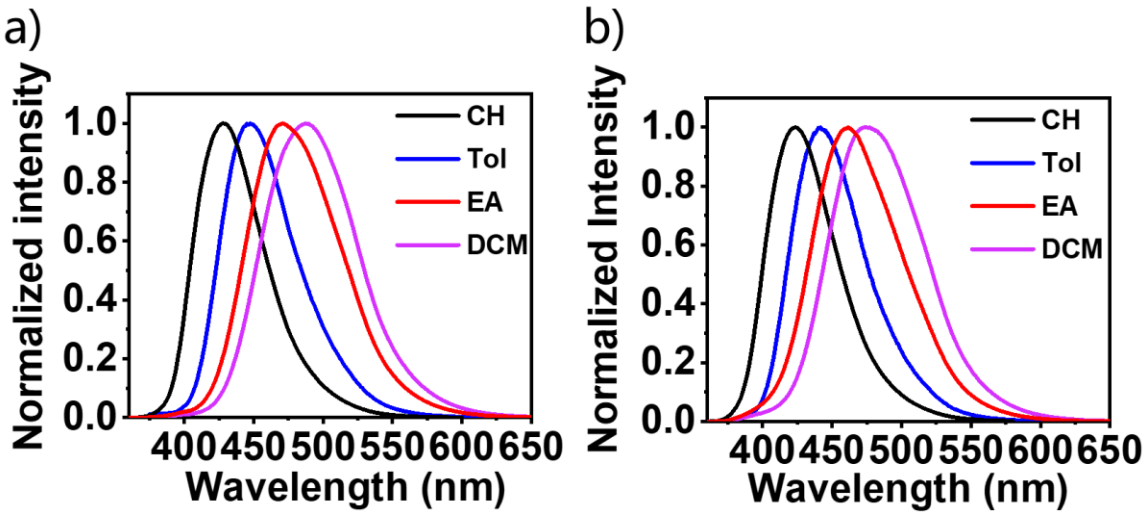

Fig. S13 The fluorescence spectra of 10^{-5} M DPS-SAIA (a) and Me-DPS-SAIA (b) in cyclohexane (CH), toluene (Tol), ethyl acetate (EA), and dichloromethane (DCM) solutions.

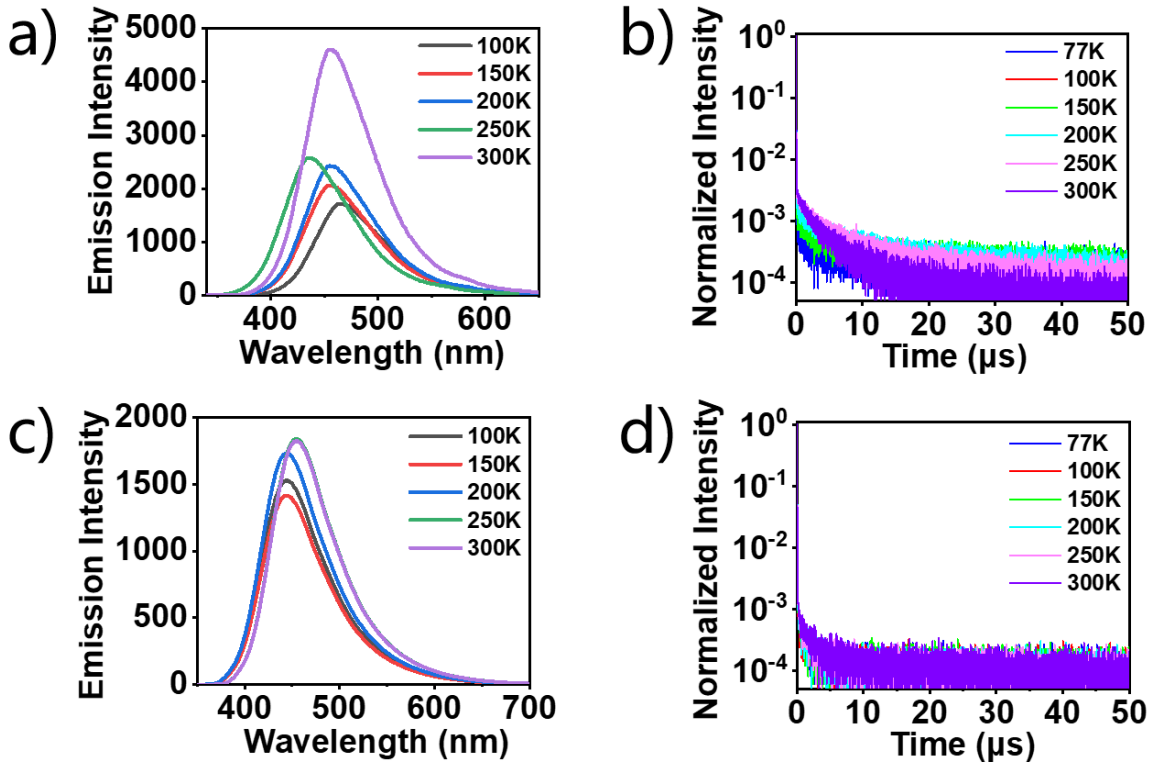

Fig. S14 The steady and transient photoluminescence spectra of DPS-SAIA and Me-DPS-SAIA in 12 wt.% doped DPEPO host at different temperature.

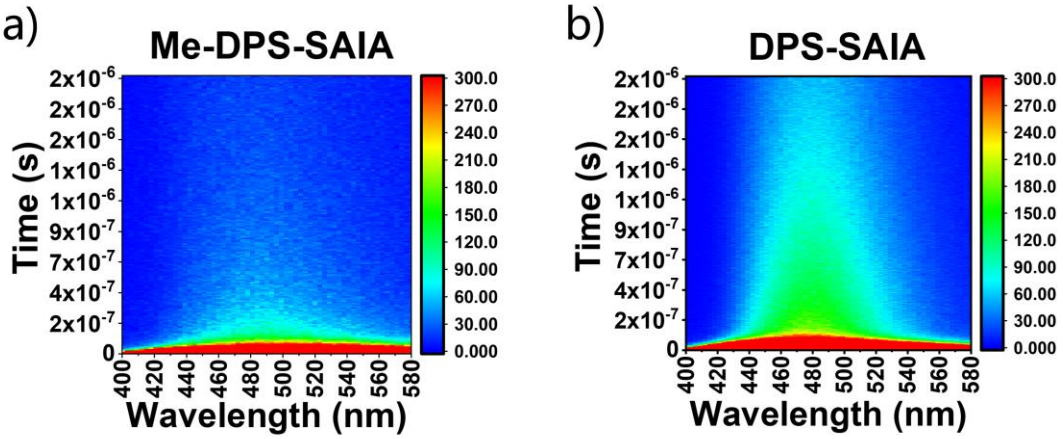

Fig. S15 The time-resolved luminescence spectra of 12 wt% Me-DPS-SAIA (a) and DPS-SAIA (b) doped in DPEPO film.

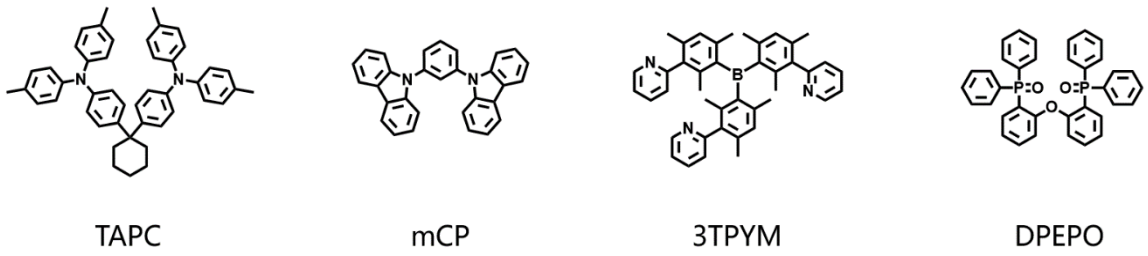

Fig. S16 The chemical structures of the materials used in the devices.

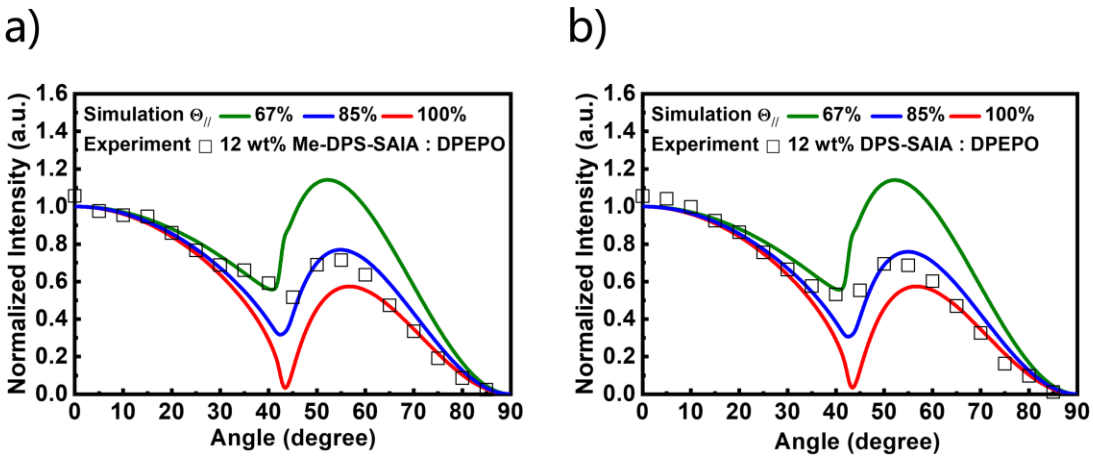

Figure S17. The measured *p*-polarized photoluminescence intensity (at emission peak wavelength) of 12 wt% Me-DPS-SAIA a) and DPS-SAIA b) doped DPEPO films. The simulated green, blue and red curves represent the results of 100%, 85% and 67% horizontal dipole ratios, respectively.

References:

[1] Pan K-C, Li S-W, Ho Y-Y, Shiu Y-J, Tsai W-L, Jiao M, et al. Efficient and Tunable Thermally Activated Delayed Fluorescence Emitters Having Orientation-Adjustable CN-Substituted Pyridine and Pyrimidine Acceptor Units. *Adv. Funct. Mater.* **2016,** *26*, 7560-7571.